FEBS Open Bio 3 (2013) 421–427

journal homepage: www.elsevier.com/locate/febsopenbio

Identification and characterization of a matrix protein (PPP-10) in the periostracum of the pearl oyster, *Pinctada fucata*

Seiji Nakayama[a,1], Michio Suzuki[a,b,1], Hirotoshi Endo[a], Kurin Iimura[a], Shigeharu Kinoshita[c], Shugo Watabe[c], Toshihiro Kogure[b], Hiromichi Nagasawa[a,*]

[a] *Department of Applied Biological Chemistry, Graduate School of Agricultural and Life Sciences, The University of Tokyo, 1-1-1 Yayoi, Bunkyo-ku, Tokyo 113-8657, Japan*
[b] *Department of Earth and Planetary Science, Graduate School of Science, The University of Tokyo, 7-3-1 Hongo, Bunkyo-ku, Tokyo 113-0033, Japan*
[c] *Department of Aquatic Bioscience, Graduate School of Agricultural and Life Sciences, The University of Tokyo, Bunkyo-ku, Tokyo 113-8657, Japan*

ARTICLE INFO

Article history:
Received 20 August 2013
Received in revised form 1 October 2013
Accepted 1 October 2013

Keywords:
Biomineralization
Chitin
Matrix protein
Periostracum
Pinctada fucata

ABSTRACT

The periostracum is a layered structure that is formed as a mollusk shell grows. The shell is covered by the periostracum, which consists of organic matrices that prevent decalcification of the shell. In the present study, we discovered the presence of chitin in the periostracum and identified a novel matrix protein, *Pinctada fucata* periostracum protein named PPP-10. It was purified from the sodium dodecyl sulfate/dithiothreitol-soluble fraction of the periostracum of the Japanese pearl oyster, *P. fucata*. The deduced amino acid sequence was determined by a combination of amino acid sequence analysis and cDNA cloning. The open reading frame encoded a precursor protein of 112 amino acid residues including a 21-residue signal peptide. The 91 residues following the signal peptide contained abundant Cys and Tyr residues. PPP-10 was expressed on the outer side of the outer fold in the mantle, indicating that PPP-10 was present in the second or third layer of the periostracum. We also determined that the recombinant PPP-10 had chitin-binding activity and could incorporate chitin into the scaffolds of the periostracum. These results shed light on the early steps in mollusk shell formation.

1. Introduction

Mollusks have shells that contain calcium carbonates and a few organic matrices, which protect their soft bodies. The periostracum is the outermost layer. It is thin and uncalcified and consists mostly of organic materials (Fig. 1). The periostracum has several functions necessary for the survival of mollusks. It provides the organic basis for initial mineral deposition at the edge of the shell [1,2]. In some species of mollusks, the periostracum itself is incorporated into the growth front of the prismatic layer, which is the outer layer of the calcified shell [1,3,4]. The periostracum also encloses the extrapallial space between the mantle and the shell and separates the extrapallial fluid from the external environment for the shell calcification [5]. Furthermore, it works as a waterproof layer that protects the shell from acids in the environment.

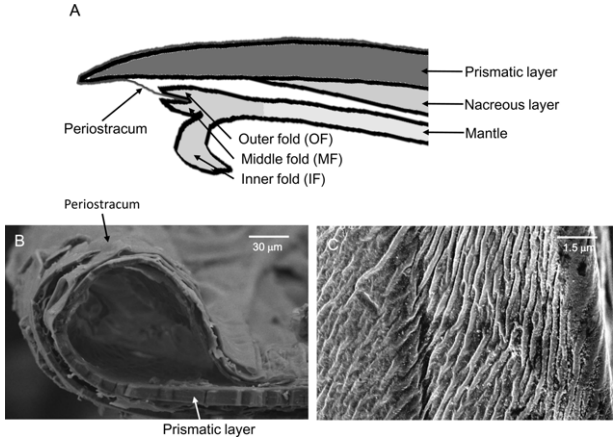

Fig. 1. (A) A schematic representation of the periostracum with the shell and the mantle of *P. fucata*. (B) An SEM image of the tip of shell growth covered by the periostracum. This image is from [4] with permission. (C) An SEM image of the inner surface of the periostracum.

Abbreviations: DOPA, 3,4-dihydroxyphenylalanine; DTT, dithiothreitol; HPLC, high performance liquid chromatography; PPP, *Pinctada fucata* periostracum protein; SDS, sodium dodecyl sulfate.

[1] These authors contributed equally to this work.

* Corresponding author. Tel.: +81 358 415 132.
E-mail address: anagahi@mail.ecc.u-tokyo.ac.jp (H. Nagasawa).

http://dx.doi.org/10.1016/j.fob.2013.10.001

The periostracum of most mollusk species consists of three morphologically distinguishable layers. The observations with the optical microscope revealed that the outer and middle layers are formed within the periostracal groove from the innermost row of cells in the outer mantle fold called basal cells [6–9], and the inner layer is secreted by the mantle epithelium [10,11]. The ultrastructural morphology of the cells and the cellular mechanisms involved in this process were described previously [3,7,12,13]. The middle layer is responsible for the secretion of the outer shell layer with vacuolization and antrum formation in bivalves [14,15]. The inner periostracum may become the organic basis for the calcification of the inner layer of the shell [14,15].

Previous work showed that the periostracum is composed of quinone-tanned proteins, mucopolysaccharides, and lipids [11]. Using a chitosan test, Peters showed that the periostracum in some species of mollusks contains chitin as the organic framework [16]. Waite et al. purified periostracin from the periostracum of the edible mussel, *Mytilus edulis*. Periostracin is a basic, water-insoluble protein with a molecular mass of 20 kDa and a unique amino acid composition consisting of 55% Gly, 10% Tyr, and 2.2% 3,4-dihydroxyphenylalanine (DOPA) [17]. DOPA in periostracin links to tyrosyl residues in the matrix proteins through a tyrosinase activity. However, the amino acid sequence of periostracin has not yet been determined. In addition, the detailed structure of the organic components and the interactions between chitin and matrix proteins are unclear.

To determine how the periostracum is formed and how it functions, we identified the *Pinctada fucata* periostracum-specific protein (PPP-10) from the Japanese pearl oyster *P. fucata*, determined the primary amino acid sequence, and discovered the chemical properties and the sites of expression of *ppp-10*.

2. Results

2.1. Identification of chitin in the periostracum

In order to identify chitin in the periostracum, alkali-insoluble materials from the periostracum were analyzed using IR and ^{1}H NMR spectra. To remove proteins exhaustively from the insoluble organic matrices, they were treated with 1 M sodium hydroxide at 105 °C for 4 h. The IR spectrum (700–2200 cm^{-1}) of the insoluble material was almost identical to that of the alkali-treated authentic chitin (Fig. 2). The absorption pattern of the sample 950–1200 cm^{-1} was very close to the characteristic pattern of chitin, although the absorption peak at 1500 cm^{-1} was broader than that of authentic chitin, possibly due to contamination principally by calcium carbonate crystals, which have an absorption around 1450 cm^{-1}. Some absorptions in the area of 700–1700 cm^{-1} may be derived from various bonds of sugars, such as C–O, C–N, N–H and C ═O. However, it is difficult to show that each absorption in the region of 900–1450 cm^{-1} is assigned to anyone of these bonds, because this region in IR spectrum is called the finger print region. The clear absorptions assigned to amide 1 and amide 2 absorptions of proteins were not observed in the spectrum of this sample, perhaps because we pre-treated the sample with NaOH to remove most proteins. These data suggested that the major component of alkali-treated insoluble organic matrices from the periostracum was probably chitin.

To gain a more precise identification of chitin, insoluble organic matrices pre-treated with aqueous sodium hydroxide and authentic chitin were separately hydrolyzed in hydrochloric acid. The ^{1}H NMR spectrum (3.0–4.0 ppm) of the hydrolysate of the insoluble material was almost identical to that of amixture of α- and β-D-glucosamine hydrochlorides and the authentic chitin hydrolysate (Fig. 3). These findings suggested that chitin existed in the periostracum as an insoluble organic matrix.

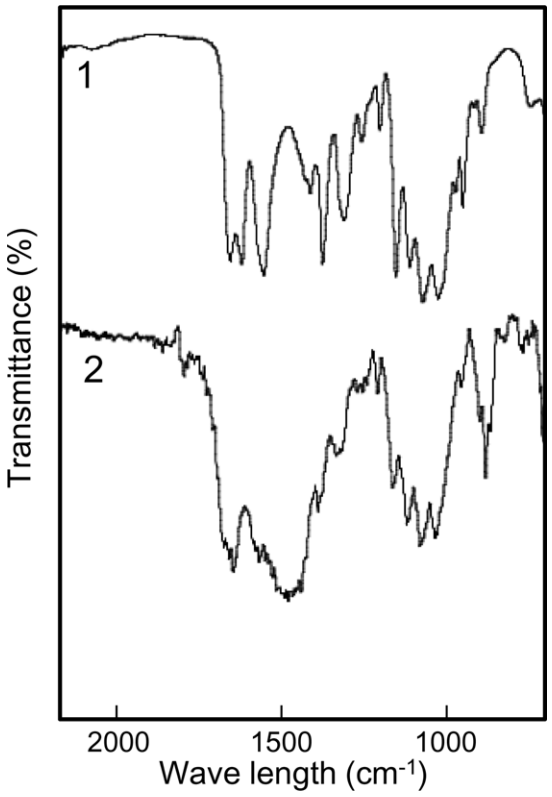

Fig. 2. The IR spectra (700–2200 cm^{-1}) of alkali-treated authentic chitin (1) and alkali-insoluble organic matrices from the periostracum (2).

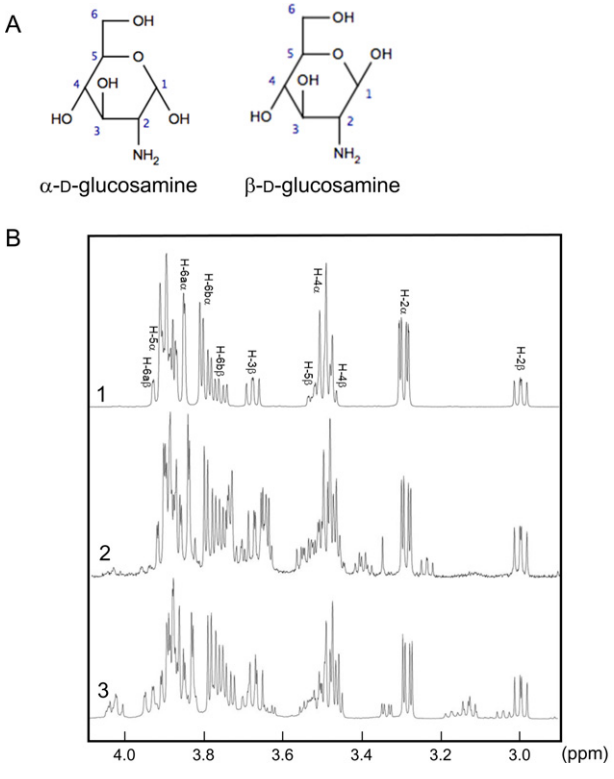

Fig. 3. (A) The chemical structures of α- and β-D-glucosamine. (B) ^{1}H NMR spectra (2.9–4.1 ppm) of D-glucosamine hydrochloride (1), acid hydrolysate of authentic chitin (2), and acid hydrolysate of alkali-insoluble organic matrices from the periostracum (3).

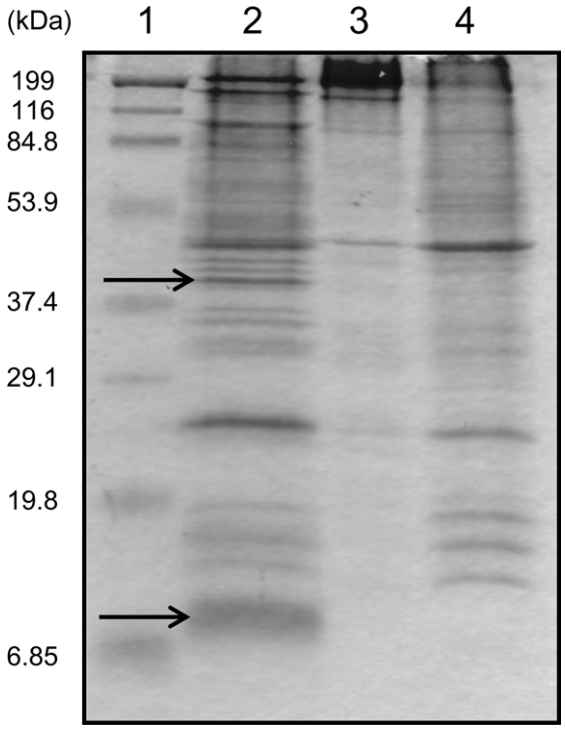

Fig. 4. SDS–PAGE of the samples from the periostracum and the body fluid. Lane 1: molecular weight markers. Lane 2: the SDS/DTT-soluble organic matrices from the periostracum. Lane 3: the soluble supernatant from the body fluid. Lane 4: the SDS/DTT-soluble organic matrices from the body fluid. Arrows indicate the 40 and 10 kDa bands that are specific to the periostracum.

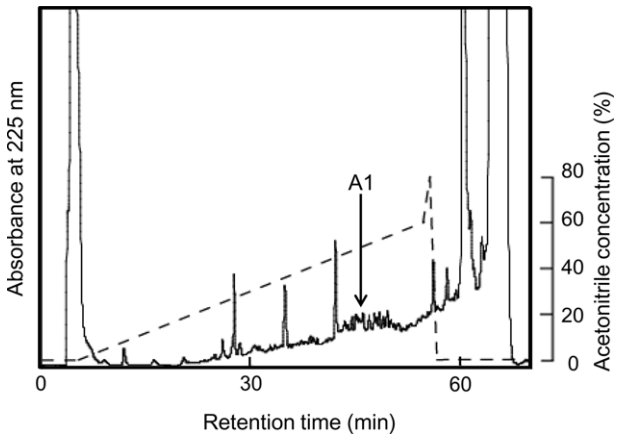

Fig. 5. The elution profile of endoproteinase Asp-N digests of the SDS/DTT-soluble organic matrices from the periostracum on RP HPLC. The broken line indicates the concentration of acetonitrile (%). The arrow indicates the fraction containing the A1 fragment.

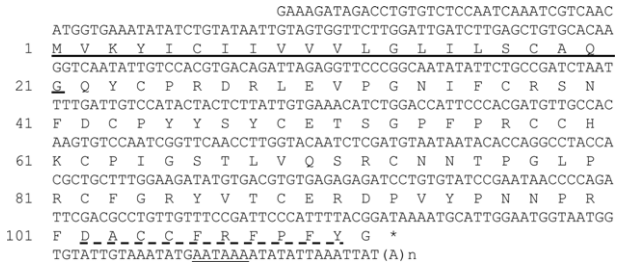

Fig. 6. The nucleotide sequence and the deduced amino acid sequence of *ppp-10*. The thick solid line indicates the signal peptide. The broken line shows the sequence of the A1 fragment. The thin solid line shows the polyadenylation signal. The nucleotide sequence of PPP-10 was registered at the DNA Data Bank of Japan with AB823700.

Fig. 7. Sequence alignment of PPP-10 with the homologous protein PUSP17 (accession number: H2A0M8) in *P. margaritifera*. Black boxes indicate identical amino acid residues. Alignment was performed by CLUSTAL W.

2.2. Extraction of matrix proteins from the periostracum

The periostracum was collected from the inner surface of the prismatic layer of the shell with viscous body fluid intact, because the adductor muscle was cut off to open the shell. To identify the periostracum-specific matrix proteins, the periostracum with the body fluid attached and the body fluid alone were boiled in the SDS/DTT solution. Both extracts were analyzed by SDS–PAGE. Two bands, 10 and 40 kDa, were detected in the periostracum extract after CBB staining but not in that of the body fluid sample (Fig. 4). We tried to determine the whole amino acid sequence of the matrix protein around 10 kDa in SDS–PAGE, but the N-terminal amino acid sequence analysis did not produce clear results, indicating that the N-terminal amino acid might be blocked by a certain posttranslational modification. To obtain further sequence information, we digested the band material with endoproteinase Asp-N in the SDS–PAGE gel and separated the products by RP HPLC (Fig. 5). The digestion produced many fragments and using amino acid sequence analysis we identified 10 amino acid residues of fragment A1, DAXXFRFPFY, where X could not be identified.

The amino acid sequence of A1 was queried in the database for *P. fucata* and it showed high similarity to the deduced amino acid sequence of 000048 from the gene database of the mantle edge and pallium. Using two primers designed to the nucleotide sequence of 000048, we amplified a partial cDNA sequence that encoded the entire open reading frame (ORF) of the matrix protein around 10 kDa and 5′-UTR by RT-PCR. We named this protein *Pinctada fucata* periostracum protein-10, PPP-10. The complete cDNA consisted of 431 bp containing a 36 bp 5′-UTR, a 336 bp ORF, a stop codon (TAA), and a 56 bp 3′-UTR. The 3′-UTR contained a canonical polyadenylation signal (AATATA) and a poly (A) tail. The deduced amino acid sequence for the PPP-10 cDNA is shown in Fig. 6. The first 21 N-terminal amino acids included a high proportion of hydrophobic residues, which suggested that it corresponds to a signal peptide. The amino acid residue following the signal peptide is glutamine. Since the glutamine residue at the N-terminus becomes pyroglutamic acid, the analysis of N-terminal amino acid sequence might be blocked due to the lack of a free amino group. PPP-10 had a calculated isoelectric point (pI) of 7.98 and a molecular mass (MM) of 10.6 kDa consisting of 91 amino acid residues. The 10 kDa molecular size estimated from the SDS–PAGE gel corresponded to the theoretical size. The conserved domain search showed that PPP-10 did not contain any conserved domains. Additionally, PPP-10 contained 14 cysteine residues that might contribute to disulfide bridge formation and the three-dimensional structure of the protein.

To find PPP-10 homologs from closely related species, we used the BLAST search against the gene database of *Pinctada margaritifera* [18]. Only prism uncharacterized shell protein 17 (PUSP17) was identified as a homologue of PPP-10 [19]. The alignment of PPP-10 and PUSP17 showed that the Cys residues were completely conserved, indicating that these proteins have similar three-dimensional structure and function (Fig. 7).

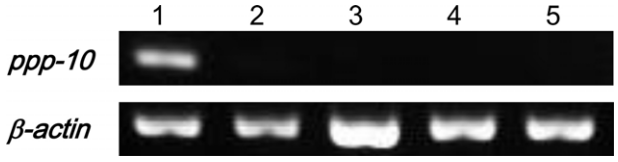

Fig. 8. Tissue-specific expression of *ppp-10* by RT-PCR analysis. cDNAs prepared from the mantle edge (lane 1), the mantle pallial (lane 2), muscle (lane 3), gill (lane 4) and midgut (lane 5) were separately subjected to RT-PCR, and the products were analyzed on an agarose gel. The expression of the *β-actin* gene was analyzed in parallel as a control.

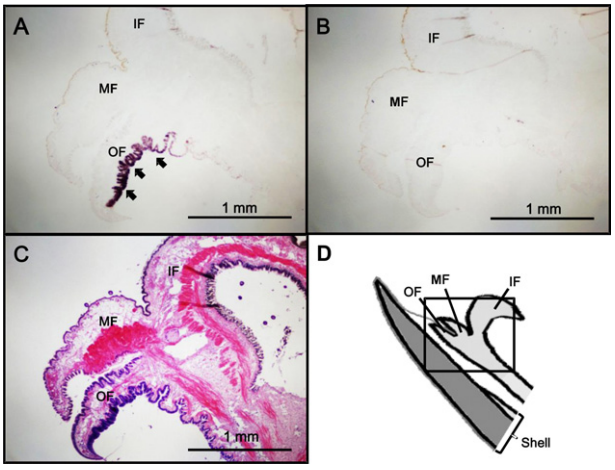

Fig. 9. Detection of *ppp-10* mRNA in the mantle of *P. fucata* by *in situ* hybridization. (A) Hybridization with the anti-sense probe at the outer side of the OF as indicated by arrows. (B) The control section stained with a sense probe. (C) The whole mantle stained with Hematoxylin–Eosin. (D) A schematic representation of the mantle and the shell.

2.3. Tissue-specific gene expression analysis

Using RT-PCR and RNA from the mantle edge, the mantle pallial, the muscles, the gills, and the midgut of *P. fucata*, we examined the tissue-specific expression of *ppp-10*. Expression of *ppp-10* was only detected in cDNA from the mantle edge, which contacts the periostracum and the prismatic layer (Fig. 8). These data suggests that PPP-10 is very likely secreted from the mantle edge and plays a role in both the periostracum formation and the calcified prismatic layer formation.

2.4. ppp-10 mRNA expression at the mantle edge

To determine the more precise expression sites of *ppp-10* mRNA in the mantle tissue of *P. fucata*, *in situ* hybridization was performed with paraffin sections. The tip of the mantle is divided into three parts, the outer fold (OF), the middle fold (MF), and the inner fold (IF) (Figs. 1A, 9C and D). The hybridization signals for *ppp-10* mRNA detected at the outer epithelial cells of the outer fold were strong, indicating that PPP-10 was secreted from the epithelium of the outer fold to the periostracum (Fig. 9A). No hybridization signal was detected at the middle fold, inner fold, or the mantle pallium. Hybridization with a control sense probe gave no significant signal (Fig. 9B).

2.5. Expression and purification of rPPP-10

To examine the chitin-binding ability of PPP-10, we prepared a recombinant protein of PPP-10 (rPPP-10). After *Escherichia coli* cells containing the expression plasmid construct were cultured, harvested, and sonicated, soluble and insoluble fractions were obtained. On the SDS–PAGE gel, the majority of rPPP-10 was detected in the insoluble

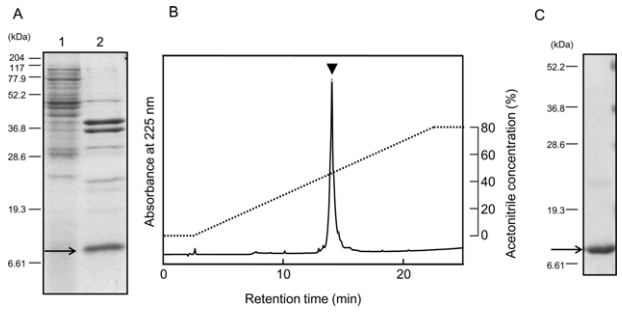

Fig. 10. Expression and purification of rPPP-10. (A) The SDS–PAGE gel of proteins including the recombinant protein of PPP-10 (rPPP-10) expressed in *E. coli* with CBB staining. Lane 1: the soluble fraction after cell breakage. Lane 2: the insoluble fraction after cell breakage. (B) The RP HPLC elution profile of rPPP-10 after the refolding reaction. The arrow indicates the purified rPPP-10 peak with normal folding form. The concentration of acetonitrile is indicated by the dotted line. The detailed chromatographic conditions are given in Experimental. (C) The SDS–PAGE gel of the refolded rPPP-10 purified by RP HPLC stained with CBB.

fraction (Fig. 10A). Therefore, the inclusion bodies were solubilized in 8 M urea solution. The resulting solution was purified using RP HPLC. The N-terminal amino acid sequence of the purified protein was found to be identical to that predicted from the cDNA sequence of rPPP-10. rPPP-10 thus purified was sparingly soluble in a buffer solution, but after the refolding reaction by the conventional method it changed to be much more soluble, suggesting successful refolding. We purified the refolded rPPP-10, and it produced a sharp peak on RP HPLC and a sharp band around 10 kDa on SDS–PAGE (Fig. 10B and C).

2.6. Chitin-binding ability of rPPP-10

An *in vitro* chitin-binding assay using refolded rPPP-10 was performed. A solution of rPPP-10 and powdered chitin were incubated together and the insoluble material including unbound chitin was successively washed with distilled water, NaCl (0.2 M), acetic acid (0.1 M), and 2% SDS in 20% 2-mercaptoethanol. Each wash was examined by SDS–PAGE. The results showed that only the SDS/2-mercaptoethanol wash contained a clear band, indicating that the rPPP-10 bound tightly to chitin (Fig. 11).

3. Discussion

In this study, we discovered that chitin was included in the organic framework of the periostracum and determined the complete cDNA sequence of the periostracum-specific matrix protein, PPP-10.

Previous work showed that the calcified shell contained chitin serving as an organic scaffold. In the nacreous layer, which is the inner layer of the calcified shell in *P. fucata*, chitin served as the major component of the organic framework, building up the compartment structure [20,21]. IR and ^{1}H NMR spectral analyses showed that the insoluble organic matrices from the prismatic layer of *P. fucata* also contained chitin [22]. On the other hand, only a few previous works showed that chitin was also identified from the periostracum of some mollusk species using XRD spectra and chitosan test [16]. In this report, we showed that the insoluble fraction from the periostracum probably contains chitin by IR and ^{1}H NMR spectral analyses. SEM images of the periostracum indicated that it was composed of an organic fibrous structure similar to chitin fibers in the exoskeleton of crustaceans, suggesting that the organic fibrous structure in the periostracum probably consisted of chitin and matrix proteins.

Matrix proteins that interact with chitin have important roles in forming the organic framework of biominerals. The fibers of the exoskeletons of crustaceans contain chitin and matrix proteins that have a Rebers–Riddiford (RR) chitin-binding concensus motif [23]. CAP-1, CAP-2, Casp-2 and SCBP-1 have the RR consensus motif and were

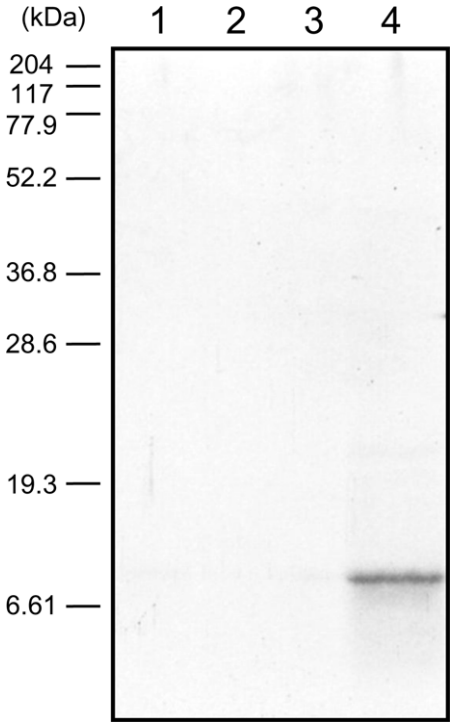

Fig. 11. Chitin-binding assay. Lane 1: water wash. Lane 2: 0.2 M NaCl wash. Lane 3: 1.0 M acetic acid wash. Lane 4: SDS/2-mercaptoethanol wash.

identified from the exoskeleton of the crayfish [24–27]. The aromatic amino acids in the β-sheet structure of the RR consensus motif bind to chitin through hydrophobic interactions [28]. CAP-1 also has an acidic region in the C-terminal domain that has the ability to interact with calcium carbonate [29]. These results indicate that CAP-1 works as a mediator between chitin and calcium carbonates. On the other hand, SCBP-1 only has the RR consensus motif but does not contain any acidic regions, indicating that SCBP-1 forms the basis of the framework as a matrix protein [27]. In the mollusk shell, Pif identified from the nacreous layer of *P. fucata* has the peritrophin A-type chitin-binding domain [30]. Prismalin-14, a matrix protein identified from the prismatic layer of *P. fucata*, contains a GY-rich region, which has chitin-binding activity [31]. However, no matrix proteins that interact with chitin have been identified from the periostracum. To reveal the structure of the matrix protein that interacts with chitin in the periostracum, we determined the whole sequence of the matrix protein in the periostracum of *P. fucata* and analyzed its localization and function.

Because the periostracum of *P. fucata* is a very thin membrane, most of the periostracum on the outside of the shell is eroded. We used the wet membranous periostracum located on the surface of the prismatic layer of the pearl oyster. However, the fresh wet periostracum was contaminated with body fluid. To search the periostracum-specific matrix proteins, we compared the extract from the fresh periostracum with that of the body fluid. Although there are some periostracum-specific matrix proteins in the SDS/DTT extract, we focused on the 10-kDa protein (PPP-10) in this report. The fact that pyroglutamic acid generally protects proteins from enzymatic degradation suggests that PPP-10 may be present in the organic framework of the extracellular matrix to preserve the shell surface. We also noted that PPP-10 has many Tyr residues as an aromatic amino acid residue. Since the aromatic amino acid residue interacts with polysaccharides such as chitin [32], we assayed chitin-binding ability of PPP-10. The results of the chitin-binding experiment showed that PPP-10 has a strong chitin-binding ability. On the other hand, PPP-10 does not contain any acidic regions that may interact with calcium carbonates. The calcium-organic interaction is attributed to acidic residues in the organic matrices, indicating that the organic matrices without any acidic regions may be scaffold molecules to make the organic basis or to support the formation of the organic microstructure. These results suggest that PPP-10 probably assists in the self-organization of the periostracum in the extracellular environment using these molecular properties. Previous work suggested that sclerosis of the periostracum was due to the oxidation of DOPA and Tyr [11,17], because the amino acid composition analysis showed that DOPA residues (2.2%) are included in periostracin. However, there are no reports identifying the primary sequences of matrix proteins in the periostracum. The determination of the whole amino acid sequence of PPP-10 will help uncover the sclerosis mechanism in the periostracum.

The outer fold of the mantle edge mainly attached to the shell surface is supposed to secrete the components of outer calcified layer of the shell. The middle fold has sensory cells to detect photic stimulation. The inner fold regulates the quantity of water that flows into the mantle cavity. The periostracum is formed within the periostracal groove between the outer and middle folds. The periostracum consists of three layers as described in Introduction. The thickness of the second and the third layers increases with the growth of the periostracum, indicating that the components of the second and third layers may be provided by the outer epithelium of the mantle [15]. *In situ* hybridization experiments revealed that *ppp-10* was expressed at the outer epithelium of the outer fold of the mantle, suggesting that PPP-10 may be included in the second and third layers. To examine this hypothesis, precise localization analysis of PPP-10 in the periostracum using antibodies is required.

The periostracum of some mollusks protects the calcified shell surface from erosion and environmental factors. However, the periostracum of *P. fucata* does not seem to work as a barrier for the shell, because it is very thin. This observation suggested that the periostracum might first of all present another key function such as serving as a scaffold for the initial calcification of the outer layer. The periostracum is incorporated in the prismatic layer as one of the components. Optical and electron microscopic observations in previous works showed very thin calcite crystals, which have oriented crystal axes were formed in the periostracum [4,15]. Although PPP-10 does not seem to be involved in calcification, other unidentified proteins in the periostracum may have important roles in the initiation of calcification of the shell. To reveal the initial calcification process of mollusk shells, further research and identification of other matrix proteins in the periostracum is needed.

4. Materials and methods

4.1. Animals and collection of the periostracum

The *P. fucata* pearl oysters were cultured by the Fisheries Research Institute, Mie Prefecture, Japan at the Ago Bay (Mie Prefecture, Japan). Live animals were sent to our laboratory in Tokyo and stored at −20 °C to collect the periostracum. RNA samples for cDNA synthesis and mantle tissues for *in situ* hybridization were prepared from live pearl oysters.

4.2. Infrared (IR) spectral analysis

The acid-insoluble material from the periostracum and authentic chitin (Wako, Tokyo, Japan) were treated separately in 1 M NaOH at 90 °C for 5 h, and the resulting insoluble organic materials were washed with distilled water. Alkali-insoluble materials were freeze-dried. The IR spectra of these samples were measured on an FT-IR (IRT-3000, JASCO, Tokyo, Japan).

4.3. NMR spectral analysis

Alkali-insoluble organic matrices from the periostracum and alkali-treated chitin were prepared by the procedure used for IR spectral analysis then were hydrolyzed in 4 M HCl at 105 °C for 4 h. The hydrolysate was concentrated *in vacuo* and lyophilized to remove the HCl. The ^{1}H NMR spectra of the two lyophilized hydrolysates and D-glucosamine hydrochloride were measured at 500 MHz in D_2O (Merck, Darmstadt, Germany) on a JEOL JNM-A500 FT-NMR system (JEOL, Tokyo, Japan).

4.4. Extraction of the matrix proteins from the periostracum

The collected periostracum was washed with distilled water and treated with 1% SDS/10 mM dithiothreitol (DTT)/50 mM Tris–HCl (pH 8.0) at 100 °C for 10 min. Extracts from body fluid were obtained in a similar manner. After desalting and concentration with ultrafiltration (Ultrafree, M. W. 10,000 cut off, Merck Millipore, Billerica, MA, USA), the solubilized extracts were separated on SDS–PAGE (15%) gels and were stained with Coomassie Brilliant Blue (CBB).

4.5. Sequence analysis of P. fucata PPP-10

The periostracum-specific band at about 10 kDa was cut out of the SDS–PAGE gel, minced, and digested with endoproteinase Asp-N (Roche, Basel, Switzerland) in 500 μL of 10% acetonitrile/1% Triton X-100/20 mM Tris–HCl (pH 8.0) for 12 h at 37 °C. The digests were run on a reversed-phase high-pressure liquid chromatography (RP HPLC) column to separate the digested peptides as described previously [28]. The purified peptide was sequenced by N-terminal amino acid analysis on a protein sequencer (492HT, Applied Biosystems, Foster City, CA, USA).

4.6. Database searching and cDNA cloning

The partial amino acid sequence (A1) of PPP-10 was searched using the basic local alignment search tool (BLAST) and the *P. fucata* databases [33]. First-strand cDNA was synthesized with 1 μg of total RNA using a SMART™ RACE cDNA Amplification kit (Clon-Tech, Palo Alto, CA, USA) according to the manufacturer's instructions. For reverse transcription (RT)-PCR, two primers were designed based on the nucleotide sequence that was identified from the *P. fucata* gene database. The first-strand cDNA was used as a template for primers PPP-F (5′-GAAAGATAGACCTGTGTCTCCAATC-3′) and PPP-R (5′-ATTTACAATACACCATTACCATTCC-3′). The round of PCR had 35 cycles of the following conditions: 30 s at 94 °C (3 min 30 s for the first cycle), 30 s at 55 °C, and 3 min at 72 °C (7 min for the last cycle).

A cDNA fragment encoding the 5′-region of PPP-10 was amplified using primers NUP (5′-AAGCAGTGGTATCAACGCAGAGT-3′) and PPP-R. The 5′ RACE was performed with 5 cycles of 5 s at 94 °C and 3 min at 72 °C; 5 cycles of 5 s at 94 °C, 10 s at 70 °C, and 3 min at 72 °C; and 25 cycles of 5 s at 94 °C, 10 s at 68 °C, and 3 min at 72 °C.

The sequences amplified by PCR were cloned into pGEM-T (Easy) Vectors (Promega, Madison, WI, USA) and were analyzed with DNA sequencing (ABI PRISM 310, Applied Biosystems, Foster City, CA, USA).

4.7. Tissue-specific expression analysis with RT-PCR

Total RNA from the mantle edge, the mantle pallial, gill, muscles, and digestive tissues were used for first-strand cDNA synthesis as described above. First strand cDNA was used as template for RT-PCR with primers PPP-RT5 (5′-GACCTGTGTCTCCAATCAAATC-3′) and PPP-RT3 (5′-ACACCATTACCATTCCAATGC-3′). Total RNA from each tissue was estimated based on the PCR product for actin, which was amplified using the primers actin-F (5′-TGTACGCTTCTGGTCGTACC-3′) and actin-R (5′-GACCGGACTCGTCGTATTCC-3′). The PCR had the following cycling conditions: 35 cycles of 30 s at 94 °C (3 min and 30 s for the first cycle), 30 s at 55 °C, and 30 s at 72 °C (3 min and 30 s for the last cycle). The PCR products were separated on a 2.0% agarose gel and stained with ethidium bromide.

4.8. In situ hybridization

In situ hybridization of PPP-10 mRNA was performed on paraffin sections. Sense and antisense digoxigenin (DIG)-labelled RNA probes were transcribed *in vitro* from the cDNA encoding PPP-10 using a DIG RNA Labelling kit (Roche). The mantle tissues were fixed overnight in Bouin solution (saturated picric acid:formalin:acetic acid, 15:5:1) at 4 °C and then dehydrated in ethanol and embedded in paraffin. Cross-sections (8 μm thick) were de-paraffinized in ethanol and re-hydrated before prehybridization in ULTRAhyb (Ambion, Carlsbad, CA, USA) and then hybridized with DIG-labelled sense or antisense RNA probes (25 μg ml^{-1}). Hybridization was performed overnight at 42 °C. After hybridization, the tissue sections were washed with 50% formamide/2 × saline-sodium citrate (SSC) for 1 h and washed twice with 0.1 × SSC for 0.5 h at 58 °C. Before adding the secondary antibody, the cross-sections were incubated in blocking reagent (Roche) in 0.1 M Tris–HCl (pH 7.5) and 0.15 M NaCl for 1 h at room temperature. After blocking, the cross-sections were incubated overnight with anti-DIG-alkaline phosphatase, Fab fragments (Roche), and diluted with blocking solution to 1:1000 (v/v) at 4 °C. The reaction with alkaline phosphatase was carried out by incubation with a nitro blue tetrazolium (NBT)/5-bromo-4-chloroindol-3-yl phosphate (BCIP) stock solution (Roche) dissolved in 0.1 M Tris–HCl (pH 9.5)/0.1 M NaCl/0.05 M $MgCl_2$ for 5 h. The sections were dehydrated in ethanol, cleared in xylene and mounted with Permount (Fisher Scientific, Kanagawa, Japan).

4.9. Production of recombinant PPP-10

We prepared the recombinant PPP-10. Primers, PPP-r5 (5′-ATGCCATGGCACAATATTGTCCACGTGAC-3′) and PPP-r3 (5′-CCGCTCGAGTTATCCGTAAAATGGGAATCG-3′), were designed according to the PPP-10 cDNA sequence. To facilitate cloning, the 5′ primers contained an *Nco*I site and two additional bases to maintain the reading frame. The 3′ primers contained an *Xho*I site and a stop codon. PCR was performed with a plasmid containing the PPP-10 cDNA as a template. PCR products were cloned into pGEM-T (Easy) Vectors. The identity of the vector inserts were confirmed by DNA sequencing. Following *Nco*I/*Xho*I digestion, the insert was ligated into the *Nco*I/*Xho*I site of a pET 28c expression plasmid (Invitrogen, Carlsbad, CA, USA).

E. coli Rosetta-gami 2 (DE3) cells (Takara, Kyoto, Japan) were transformed with the expression plasmids containing the inserts and were grown on LB plates containing kanamycin (30 μg/ml). Selected colonies from each plate were grown in an LB medium containing kanamycin at 37 °C in a shaker at 150 rpm overnight. Overnight cultures were diluted 50-fold in the same LB medium and incubated at 37 °C with shaking at 150 rpm for 2 h. Isopropyl thio-b-D-galactoside (IPTG; Nacalai Tesque, Kyoto, Japan) was added to each culture to a final concentration of 1 mM and the cultures were incubated at 37 °C with shaking at 150 rpm for 2 h. Bacterial cells were harvested by centrifugation and suspended in 1/20 the volume of phosphate-buffered saline (PBS) (10 mM KH_2PO_4, 0.15 M NaCl, pH 7.5). The cells were disrupted by sonication and were centrifuged at 10,000*g* for 10 min. The supernatant was removed and the pellet was resuspended in PBS. The pellets containing the recombinant PPP-10 (rPPP-10) were solubilized in 8 M urea solution and purified by RP HPLC on a CAPCELL PAK C_8 DD column (10 × 150 mm, Shiseido, Tokyo, Japan) with a 20-min linear gradient of 0–80% acetonitrile in 0.05% trifluoroacetic acid (TFA) at a flow rate of 4.7 ml/min. The purified sample was freeze-dried.

4.10. Refolding rPPP-10

The purified rPPP-10 was suspended in a redox buffer containing 6 M guanidine hydrochloride/20 mM DTT/50 mM Tris–HCl (pH 8.8) at 4 °C for 24 h. The refolded rPPP-10 was purified by RP HPLC on a CAPCELL PAK C_{18} UG300 column (2.0 × 250 mm; Shiseido) with an 80-min linear gradient of 0–80% acetonitrile in 0.05% TFA at a flow rate of 0.2 ml/min. The purified sample was freeze-dried and stored at −20 °C until use.

4.11. Chitin-binding assay

We used the chitin-binding assay described by Inoue et al. [24] with some modifications. 5 μg of rPPP-10 were incubated with 1.5 mg of chitin (Wako, Osaka, Japan) for 12 h at room temperature. After removal of the solution by centrifugation, the insoluble material was washed twice with 300 μl of distilled water. The residue was then washed successively with 300 μl of 0.2 M NaCl and 300 μl of 0.1 M acetic acid. Each wash was passed through a Sep-Pak Plus C18 environmental cartridge (Waters, Milford, MA, USA) and was eluted with 80% acetonitrile/0.05% TFA. Each eluate was concentrated. The final residue was boiled in 30 μl of 2% SDS containing 20% 2-mercaptoethanol for 15 min and the supernatant was obtained by centrifugation for 1 min at 10,000*g*. Each eluate and the SDS extract were run on a 15% SDS–PAGE gel under reducing conditions. After electrophoresis, the gel was stained with CBB.

Acknowledgements

We are grateful to Dr. H. Aoki of the Fisheries Research Institute, Mie Prefecture, Japan, for the kind gift of live pearl oysters. We are also grateful to Dr. Y. Gueguen for support in the search for a PPP-10 homologue from the database of *P. margaritifera*. This work was supported by Grants-in-Aid for Scientific Research (17GS0311, 22248037 and 22228006) from the Japan Society for the Promotion of Science (JSPS). M. Suzuki was supported by a Research Fellowship of JSPS for young scientists.

References

[1] Taylor, J.D. and Kennedy, W.J. (1969) The influence of the periostracum on the shell structure of bivalve molluscs. Calcif. Tissue Res. 3, 274–283.
[2] Nakahara, H. and Bevelander, G. (1971) The formation and growth of the prismatic layer of *Pinctada radiata*. Calcif. Tissue Res. 7, 31–45.
[3] Wada, K. (1963) Studies on the mineralization of the calcified tissue in molluscs. 6. Crystal structure of the calcite grown on the inner surface of calcitostracum. J. Electron Microsc. 12, 224–227.
[4] Suzuki, M., Nakayama, S., Nagasawa, H. and Kogure, T. (2013) Initial formation of calcite crystals in the thin prismatic layer with the periostracum of *Pinctada fucata*. Micron 45, 136–139.
[5] Neff, J.M. (1972) Ultrastructural studies of periostracum formation in the hard shelled clam *Mercenaria mercenaria* (L). Tissue Cell 4, 311–326.
[6] Kawaguti, S. and Ikemoto, N. (1962) Electron microscopy on the mantle of the bivalved gastropod. Biol. J. Okayama Univ. 8, 1–16.
[7] Bevelander, G. and Nakahara, H. (1967) An electron microscopic study of the formation of the periostracum of *Macrocallista maculata*. Calcif. Tissue Res. 1, 55–67.
[8] Bubel, A. (1973) An electron-microscope study of periostracum formation in some marine bivalves. Mar. Biol. 20, 222–234.
[9] Richardson, C.A., Runham, N.W. and Crisp, D.J. (1981) A histological and ultrastructural study of the cells of the mantle edge of a marine bivalve, *Cerastoderma edule*. Tissue Cell 13, 715–730.
[10] Beedham, G.E. (1958) Observations on the mantle of the *Lamellia branchia*. Q. J. Microsc. Sci. 99, 181–197.
[11] Hillman, R.E. (1961) Formation of the periostracum in *Mercenaria mercenaria*. Science 134, 1754–1755.
[12] Saleuddin, A.S.M. (1974) An electron microscopic study of the formation and structure of the periostracum in Astarte (Bivalvia). Can. J. Zool. 52, 1463–1471.
[13] Salas, C., Marina, P., Checa, A.G. and Rueda, J.L. (2012) The priostracum of *Digitaria digitaria* (Bivalvia: Astartidae): formation and structure. J. Molluscan Stud. 78, 34–43.
[14] Clark, G.R. II (1974) Calcification on an unstable substrate: marginal growth in the mollusk *Pecten diegensis*. Science 183, 968–970.
[15] Checa, A. (2000) A new model for periostracum and shell formation in Unionidae (Bivalvia, Mollusca). Tissue Cell 32, 405–416.
[16] Peters, W. (1972) Occurrence of chitin in Mollusca. Comp. Biochem. Physiol. B 41, 541–550.
[17] Waite, J.H., Saleuddin, A.S.M. and Andersen, S.O. (1979) Periostracin – a soluble precursor of sclerotized periostracum in *Mytilus edulis* L. J. Comp. Physiol. 130, 301–307.
[18] Joubert, C., Piquemal, D., Marie, B., Manchon, L., Pierrat, F., Zanella-Cléon, I. et al. (2010) Transcriptome and proteome analysis of *Pinctada margaritifera* calcifying mantle and shell: focus on biomineralization. BMC Genomics 11, 613.
[19] Marie, B., Joubert, C., Tayale, A., Zanella-Cleon, I., Belliard, C., Piquemal, D. et al. (2012) Different secretory repertoires control the biomineralization processes of prism and nacre deposition of the pearl oyster shell. Proc. Natl. Acad. Sci. U.S.A. 109, 20986–20991.
[20] Zentz, F., Bedouet, L., Almeida, M.J., Milet, C., Lopez, E. and Giraud, M. (2001) Characterization and quantification of chitosan extracted from nacre of the abalone *Haliotis tuberculata* and the oyster *Pinctada maxima*. Mar. Biotechnol. (N.Y.) 3, 36–44.
[21] Nudelman, F., Shimoni, E., Klein, E., Rousseau, M., Bourrat, X., Lopez, E. et al. (2008) Forming nacreous layer of the shells of the bivalves *Atrina rigida* and *Pinctada margaritifera*: an environmental- and cryo-scanning electron microscopy study. J. Struct. Biol. 162, 290–300.
[22] Suzuki, M., Sakuda, S. and Nagasawa, H. (2007) Identification of chitin in the prismatic layer of the shell and a chitin synthase gene from the Japanese pearl oyster, *Pinctada fucata*. Biosci. Biotechnol. Biochem. 71, 1735–1744.
[23] Rebers, J.E. and Riddiford, L.M. (1988) Structure and expression of a *Manduca sexta* larval cuticle gene homologous to *Drosophila* cuticle genes. J. Mol. Biol. 203, 411–423.
[24] Inoue, H., Ozaki, N. and Nagasawa, H. (2001) Purification and structural determination of a phosphorylated peptide with anti-calcification and chitin-binding activities in the exoskeleton of the crayfish, *Procambarus clarkii*. Biosci. Biotechnol. Biochem 65, 1840–1848.
[25] Inoue, H., Ohira, T., Ozaki, N. and Nagasawa, H. (2004) A novel calcium-binding peptide from the cuticle of the crayfish, *Procambarus clarkii*. Biochem. Biophys. Res. Commun 318, 649–654.
[26] Inoue, H., Yuasa-Hashimoto, N., Suzuki, M. and Nagasawa, H. (2008) Structural determination and functional analysis of a soluble matrix protein associated with calcification of the exoskeleton of the crayfish, *Procambarus clarkii*. Biosci. Biotechnol. Biochem. 72, 2697–2707.
[27] Suzuki, M., Sugisaka-Nobayashi, A., Kogure, T. and Nagasawa, H. (2013) Structural and functional analyses of a strong chitin-binding protein-1 (SCBP-1) from the exoskeleton of the crayfish *Procambarus clarkii*. Biosci. Biotechnol. Biochem. 77, 361–368.
[28] Iconomidou, V.A., Willis, J.H. and Hamodrakas, S.J. (1999) Is beta-pleated sheet the molecular conformation which dictates formation of helicoidal cuticle? Insect Biochem. Mol. Biol. 29, 285–292.
[29] Inoue, H., Ohira, T. and Nagasawa, H. (2007) Significance of the N- and C-terminal regions of CAP-1, a cuticle calcification-associated peptide from the exoskeleton of the crayfish, for calcification. Peptides 28, 566–573.
[30] Suzuki, M., Saruwatari, K., Kogure, T., Yamamoto, Y., Nishimura, T., Kato, T. et al. (2009) An acidic matrix protein, Pif, is a key macromolecule for nacre formation. Science 325, 1388–1390.
[31] Suzuki, M., Murayama, E., Inoue, H., Ozaki, N., Tohse, H., Kogure, T. et al. (2004) Characterization of Prismalin-14, a novel matrix protein from the prismatic layer of the Japanese pearl oyster (*Pinctada fucata*). Biochem. J. 382, 205–213.
[32] Elgavish, S. and Shaanan, B. (1997) Lectin–carbohydrate interactions: different folds, common recognition principles. Trends Biochem. Sci. 22, 462–467.
[33] Kinoshita, S., Wang, N., Inoue, H., Maeyama, K., Okamoto, K., Nagai, K. et al. (2011) Deep sequencing of ESTs from nacreous and prismatic layer producing tissues and a screen for novel shell formation-related genes in the pearl oyster. PLoS One 6, e21238.